CHEMISTRY OF MATERIALS

Article

pubs.acs.org/cm

Entrapment of Enzymes within Sol–Gel-Derived Magnetite

Andrey S. Drozdov,[†] Olga E. Shapovalova,[†] Vladimir Ivanovski,[‡] David Avnir,[§] and Vladimir V. Vinogradov*[,†]

[†]Laboratory of Solution Chemistry of Advanced Materials and Technologies, ITMO University, St. Petersburg, 197101, Russian Federation

[‡]Faculty of Natural Sciences and Mathematics, Institute of Chemistry, Ss. Cyril and Methodius University in Skopje, Skopje, 1000, Republic of Macedonia

[§]Institute of Chemistry and the Centre for Nanoscience and Nanotechnology, The Hebrew University of Jerusalem, Jerusalem, 91904, Israel

Supporting Information

ABSTRACT: Magnetically controlled enzymatic composites have received much attention for both therapeutic and industrial applications. Until now, such materials have been composed of at least four components: the enzyme, magnetic nanoparticles, their stabilizing components, and an organic or inorganic (or hybrid) matrix as a carrier. However, such compositions affect the magnetic response and the enzymatic activity, and also pose obstacles for intravenous administration, because of regulatory restrictions. Here, we present a methodology for the creation of magnetic bioactive nanocomposites composed of only two biocompatible components: an enzyme and magnetite nanoparticles. A series of magnetic biocomposites with a full set of therapeutical and industrial proteins (carbonic anhydrase, ovalbumin, horseradish peroxidase, acid phosphatase, proteinase, and xylanase) were successfully created by the direct entrapment of the proteins within a sol–gel magnetite matrix specially developed for these aims. The activity of the entrapped enzymes was studied at different temperatures and concentrations, and it was found that they showed remarkable thermal stabilization induced by the ferria matrix. For instance, entrapped carbonic anhydrase catalyzed the decomposition of *p*-nitrophenylacetate at a temperature of 90 °C, while free enzyme completely loses activity and denaturates already at 70 °C. Magnetic characterization of the obtained biomaterials is provided.

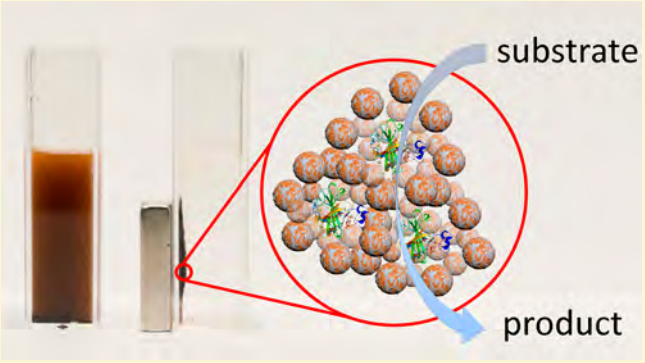

INTRODUCTION

Our current knowledge of sol–gel-derived biomaterials is largely based on the intensive studies of silica: with this oxide, methodologies of entrapment were developed, stability studies were carried out, and enzymatic activities were analyzed.[1] On the advantages side, silica sol–gel materials not only preserve the activity of the bioactive dopants, but also provide exceptional stability to a variety of proteins and bioactive molecules against various deterioration processes.[2−5] And yet, an elementary, key limitation of silica that has been a major obstacle towards development of medical applications is the fact that this oxide is not approved by medical regulators for injection. However, this limitation on sol–gel materials can be addressed if the scope is broadened beyond silica. Among the common oxides, ferria (iron oxides in general) and alumina are approved for parenteral administration into the human body.[6] Magnetite is approved as a component for magnetic resonance imaging (Refidex and Resovist),[7] and for treatment of iron deficiency (anemia) in people with chronic kidney failure (Ferumoxytol, Feraheme),[8] while alumina is the most widely used vaccine adjuvant.[9] Therefore, these two oxides are perfect candidates for the development of sol–gel-derived carriers of proteins, antibodies,[10] drugs, and other bioactive components, aimed at their stabilization, delivery, and release.

The use of the sol–gel approach for these purposes is primarily dependent on the development of biofriendly synthetic procedures for the preparation of the oxide hydrosols–alumina and ferria in our context, from which the doped sol–gel materials are obtained. In a series of recent papers, we have addressed that need by developing an ultrasonic approach for the preparation of a variety of stable oxide hydrosols, without the need for any stabilizing agents and at neutral pH, that is, highly pure oxide hydrosols composed only of the nanometric oxide particles and water.[11−13] Alumina was studied intensively by this new methodology, resulting in a series of active biomaterials with unprecedented stabilities and performances, including therapeutic[14] and biotechnological

Received: January 15, 2016
Revised: March 16, 2016
Published: March 16, 2016

DOI: 10.1021/acs.chemmater.6b00193
Chem. Mater. 2016, 28, 2248−2253

enzymes,[15] synergistically active wound-healing materials,[16] and materials with efficient thrombolytic properties.[17,18]

The time has come now to study intensively the second regulatory approved oxide, ferria (iron oxide), and, in particular, magnetite, because of its added value of magnetic maneuverability. Here, we report the first successful entrapment of enzymes within magnetite ferria, and the finding that thermal protectability, typical of sol−gel materials, is obtained with this class as well. The ability to move on to ferria became possible following a recent solution[13] of the well-known problem of ferria hydrosols: these are so unstable (because of low surface charge of the particles) that a massive use of additives or use of extreme pH values are needed in order to achieve sol stability. However, ferria hydrosols so obtained are not friendly for protein entrapment. To overcome this problem and produce magnetic responsive biomaterials, magnetite nanoparticles were coentrapped with enzymes within oxides such as silica[19] or titania,[20] or, alternatively, proteins were covalently linked to magnetite nanoparticles.[21] We have recently solved the problem of producing pure ferria hydrosols (magnetite nanoparticle and water only) avoiding stabilizing agents and retaining neutral pH. The approach, described in detail in ref 13, is a carefully tailored process that combines an unconventional nonstoichiometric Fe^{2+}/Fe^{3+} ratio, ultrasonic treatment, and the Schikorr reaction;[13] all of these cause the magnetite particles to have a positive surface charge that is high enough to allow the formation of a stable hydrosol at neutral pH.

In this report, we focus on bovine carbonic anhydrase (CAB), which is one of the most efficient and well-studied enzymes[22] and a member of an important class of enzymes used in the treatment of Alzheimer's disease.[23] Recently, CAB has also been the topic of a report on the ability of the sol−gel process to renature a thermally denatured enzyme to an enzyme with higher activity, compared to the free one (the "Phoenix effect").[24] Following the detailed study of CAB@ferria described below, which has revealed enhanced thermal stability, we screened over several proteins to test both the generality of the entrapment procedure in magnetite and the gained stability. These proteins iclude the following: ovalbumin (OVA); horseradish peroxidase (HRP), which is a member of the peroxidase enzymes family, which is used for conversion of pro-drugs to active ones; acid phosphatase (AcP), which is important for prostate cancer treatment;[25] xylanase (XY), which is a key biotechnological enzyme widely used in the paper industry and in the production of biodiesel;[26] and proteinase (PR), which is a protease-class enzyme used in the food and leather industries.[27] We believe that our report provides conclusive evidence that sol−gel-derived ferria is a matrix worthy of attention as a biocarrier of enzymes, while being, at the same time, stabilizing, magnetic, and injectable.

EXPERIMENTAL DETAILS

Chemicals. Carbonic anhydrase from bovine erythrocytes (CAB, Catalog No. C-2624), ovalbumin (OVA), horseradish peroxidase (HRP, Catalog No. P-8375), acid phosphatase from potato (AcP, Catalog No. P-0157), β-xylanase from *Trichoderma longibrachiatum* (XY), proteinase from *Aspergillus melleus* (PR), *p*-nitrophenylacetate (*p*NPA), 2,2′-azino-bis(3-ethylbenzo-thiazoline-6-sulfonic acid) (ABTS), hydrogen peroxide (30%), and *p*-nitrophenylphosphate (pNPP) were all obtained from Sigma−Aldrich. Glycine buffers were made from glycine solution (0.05 M, from Sigma−Aldrich) with a desired volume of 1 M HCl. Tris-buffer was made from 0.1 M Trizma-hydrochloride solution with a desired volume of 1 M NaOH. The hydrosol was prepared from iron(II) chloride tetrahydrate, iron(III) chloride hexahydrate, and ammonia, all from Sigma−Aldrich.

Preparation of the Protein@Ferria Biocomposites. *Ferria Pure Hydrosol.* This was prepared ultrasonically as described is ref 13. Briefly, 2.5 g of $FeCl_2 \cdot 4H_2O$ and 5 g of $FeCl_3 \cdot 6H_2O$ were dissolved in 100 mL of deionized water under constant stirring (500 rpm). Then, 12 mL of aqueous ammonia solution was added under constant stirring (500 rpm) at room temperature. Using a magnet, the formed magnetite precipitate was collected and washed with deionized water until neutral pH. The washed black precipitate was mixed with 100 mL of deionized water and subjected to ultrasonic treatment (37 kHz, 110 W) under constant stirring (300 rpm) for 120 min. The resulting magnetite sol was then cooled to room temperature. The mass fraction of the magnetite nanoparticles in the resulting sol 2.2%, with an average particle size of 10 nm, as determined from high-resolution scanning electron microscopy (HR-SEM) imaging (see Figure 1S in the Supporting Information).

CAB@Ferria. Different quantities (from 0 to 112 μL) of CAB solution (17500 U mL^{-1}) in Tris-buffer (pH 7.4) were mixed with 200 μL of freshly prepared ferria sol and dried under vacuum for 24 h. The CAB@ferria composite was rinsed with Tris-buffer (pH 7.4) solution to ensure removal of any adsorbed protein. The entrapment of CAB was full, as indicated by the lack of activity of the washings; this is true for all other enzymes in this study.

OVA@Ferria. Ten milliliters (10 mL) of the freshly prepared ferria sol was mixed with 1 mL of the protein water solution, prepared separately using 10 mg of the protein. The resulting protein-containing sol was dried in a vacuum desiccator for 24 h at room temperature. The weight content of protein in the final composites was 5%. Comparative adsorption experiments were carried out by exposing 10 mL of the same OVA solution to ferria xerogel obtained from 10 mL of 30 min ultrasonically treated ferria sol (see Figure 2S in the Supporting Information for infrared (IR) characterization and comparison to adsorption).

HRP@Ferria. Two hundred microliters (200 μL) of freshly prepared ferria sol was transferred to a cuvette, then 25 μL of HRP (20 U mL^{-1}) solution in glycine-HCl buffer (pH 4.7) was added and the resulting sol was mixed. The sol was dried under vacuum for 24 h. The HRP@ferria composite was rinsed with glycine-HCl buffer (pH 4.7) solution.

AcP@Ferria. Two hundred microliters (200 μL) of freshly prepared ferria sol was transferred to a cuvette, then 5 μL of AcP (200 U mL^{-1}) solution in glycine-HCl buffer (pH 5.0) was added and the resulting sol was mixed. The sol was dried under vacuum for 24 h. The composite was rinsed with glycine-HCl buffer (pH 5.0) solution.

Proteins@Ferria for Differential Scanning Calorimetry (DSC) Analyses. Twelve milligrams (12 mg) of the corresponding protein (CAB, OVA, HRP, AcP, XY, PR) was added to 6 mL of the sol at room temperature, so that the final fraction was 10 wt %. The suspension was aged for 3 h and dried at 20 °C for 2 days in a vacuum desiccator.

Thermal Stability of CAB@Ferria. After rinsing the bioactive hybrid (10 wt % enzyme loading) with 1 mL of Tris-buffer (pH 7.4) for 10 min, 3 mL of Tris-buffer (pH 7.4) solution was added to it and the cuvette was incubated at temperature of 65 °C for periods ranging from 4 min to 60 min. After incubation, 125 μL of pNPA solution (0.8 M in acetone) was added, and enzymatic activity was spectrophotometrically measured at 40 °C by following the formation of *p*-nitrophenolate (*p*NP) (see reaction 1 in Figure 1) through the absorption at 405 nm. Testing for possible activity of the rinsing solutions was carried out by adding 1 mL of Tris-buffer and 60 μL of *p*NPA solution to it. For comparative analysis of the free enzyme, 10 μL of the enzyme solution (17500 U mL^{-1}) and 3 mL of Tris-buffer were mixed and treated similarly to the bioactive composite.

Enzymatic Activity of the Protein@Ferria Biocomposites. *CAB@Ferria.* After rinsing the bioactive hybrid (4 mg, 12 wt % enzyme loading) with 1 mL of Tris-buffer (pH 7.4) for 10 min, 3 mL of Tris-buffer (pH 7.4) solution was added and the cuvette was incubated at temperatures ranging from 20 °C to 90 °C for 5 min. After incubation, 125 μL of *p*NPA solution (0.8 M, in acetone) was added, and the enzymatic activity was measured at the same temperature following the

DOI: 10.1021/acs.chemmater.6b00193
Chem. Mater. 2016, 28, 2248−2253

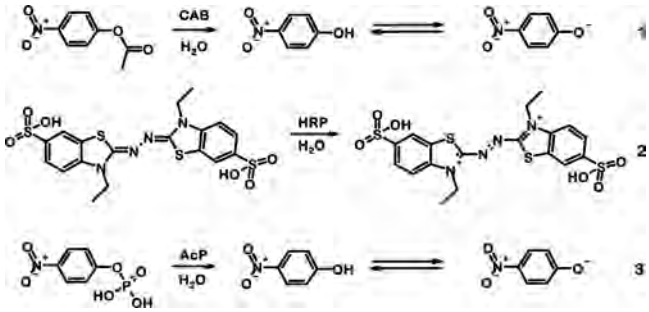

Figure 1. Enzyme-catalyzed reactions used in this study.

formation of *p*-nitrophenolate (*p*NP; reaction 1 in Figure 1) spectrophotometrically through the absorption at 405 nm. A small hydrolytic effect of the ferria matrix without enzyme was determined similarly and the enzymatic activity results were corrected accordingly (5%−10% correction, depending on the temperature of the experiment). Testing for possible activity of the rinsing solutions was carried out by adding 1 mL of Tris-buffer and 60 μL of *p*NPA solution; no activity was found. For comparative analysis of the free enzyme, 10 μL of the enzyme solution (17 500 U mL^{-1}) and 3 mL of Tris-buffer were mixed and treated similarly to the bioactive composite.

HRP@Ferria. The enzymatic activity was measured using ATBS as a substrate (reaction 2 in Figure 1). The substrate solution is composed of 0.1 mL of 30% H_2O_2 and 1 mL of 0.5 mM ABTS in 2 mL of 50 mM glycine-HCl buffer (pH 4.7). After rinsing with 1 mL of glycine-HCl buffer (pH 4.7), 4 mg of the bioactive composite containing HRP@ferria (0.3 wt % enzyme loading) was transferred into a cuvette, where 300 μL of glycine-HCl buffer (pH 4.7) was added and comparative incubation was carried out at 25 and 65 °C for 1 h. Then, 3 mL of the substrate solution was added and the enzymatic activity was followed spectrophotometrically at 420 nm and a temperature of 30 °C. Testing of possible enzymatic activity of the rinsing solutions was carried out under similar conditions: none was found. For the free enzyme, 1 μL of HRP (20 U mL^{-1}) was added to 300 μL of glycine-HCl buffer and was treated similarly to the entrapped enzyme.

AcP@Ferria. After rinsing the bioactive composite with 1 mL of glycine-HCl buffer (pH 5.0), 4 mg of it was transferred into a cuvette and 300 μL of glycine-HCl buffer (pH 5.0) was added. Comparative incubation was carried out at 25 and 65 °C for 30 min. After that, 3 mL of 10.8 mM *p*NPP solution in glycine-HCl buffer (pH 5.0) was added, and the enzymatic activity (reaction 3 in Figure 1) was measured spectrophotometrically by following the absorbance at 405 nm and a temperature of 30 °C. Rinsing solutions were tested as described above. For the free enzyme, 1 μL of AcP (200 U mL^{-1}) was added to 300 μL of glycine-HCl buffer (pH 5.0) and was treated similarly to the entrapped enzyme.

Characterization Methods. Specific surface area pore volume and pore size distribution were investigated via nitrogen adsorption at 77 K, using a Quantachrome Nova 1200e system, then analyzed by the Brunauer−Emmett−Teller (BET) and Barrett−Joyner−Halenda (BJH) equations. Prior to analysis, all samples were degassed at room temperature for 48 h. For scanning electron microscopy (SEM, using an ultra-high-resolution Magellan 400L electron microscope), the final suspension of the entrapped enzyme was coated on silicon wafer and fully dried under vacuum. The samples for TEM were obtained by dispersing a suspension drop on copper mesh covered with carbon (FEI TECNAI, Model G2 F20, at an operating voltage of 200 kV). ATR spectra were recorded on an FT-IR spectrometer system (PerkinElmer, Model 2000 FT-IR), with a Golden Gate reflectance accessory (SPECAC) equipped with diamond ATR crystal and ZnSe lenses. DSC curves were obtained with a Netzsch Model 204 F1 Phoenix apparatus and a heating rate of 10 °C min^{-1} was used from 30 °C to 150 °C under nitrogen. The spectrophotometrical measurement of enzymatic activity was carried out using an Agilent Cary HP 8454 Diode Array spectrophotometer with TEC.

RESULTS AND DISCUSSION

CAB@Ferria. As mentioned in the Introduction, the entrapment of proteins within sol−gel-derived magnetite (or, for that matter, within any form of ferria) has not been described previously. The entrapment procedure described in the Experimental Details section represents a carefully optimized method, which, as also described in the Introduction, is based on the newly developed biofriendly pure magnetite hydrosol.[12] One of the most important optimized parameters was the enzyme loading. Figure 2a shows the conversion rate

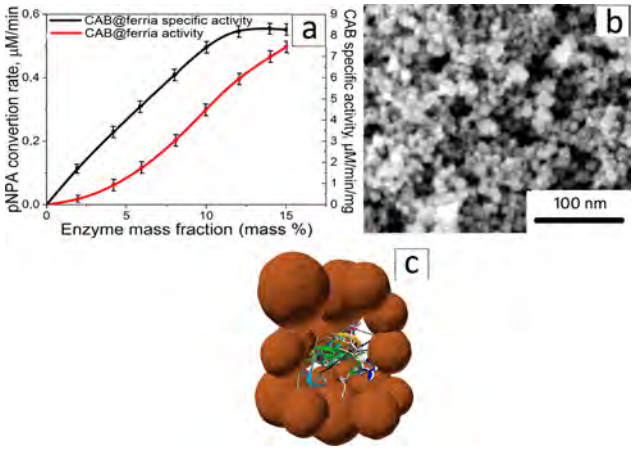

Figure 2. (a) Conversion rate (left axis) and specific enzymatic activity (right axis) of the CAB@ferria composite. (b) HR-SEM of the CAB@ferria colloid particles. (c) Model of an enzyme molecule entrapped within a matrix aggregated cage.

and specific activity of CAB@ferria, as a function of the amount of entrapped enzyme. It is seen that, while the absolute activity increases with loading, the specific activity (defined as absolute activity divided by the mass fraction of enzyme in the composite) levels off at a mass fraction of ∼12%. Such a threshold is usually indicative of the onset of formation of aggregates of the dopant;[13] that is, a larger portion of enzyme with loading beyond this threshold is buried inside the aggregates and becomes inaccessible. An approximate model estimate shows that ∼20 magnetite nanoparticles (∼10 nm in diameter, shown in Figure 2b) are needed to coat and entrap one protein molecule (6 nm × 6 nm × 24 nm;[21] see Figure 2c), that is, at higher loads there is a deficiency in nanomagnetite particles to coat each enzyme molecule individually. Therefore, 12% loading was used in the following reported measurements. The explanation of why activity with entrapped enzyme is possible at all lies in the porosity of the matrix. Typical surface areas, obtained from the BET analysis of the nitrogen adsorption isotherms, are 120 m^2/g for both the pure magnetite and for CAB@ferria, with BJH average pore diameters of 8.5 and 8.2 nm, respectively (see Figure 3S and Table 1S in the Supporting Information).

Differential scanning calorimetry (DSC) measurements of the free and entrapped enzyme provided strong indication of a thermal stability effect of the matrix. We recall that DSC has proved in a series of recent studies[11,14,15] as a perfect analytical tool for detection of thermal stabilization of entrapped enzymes; the idea has been to follow the denaturing temperature, which behaves in this analysis as any other phase transition. The results of the measurements (Figure 3a) show that the denaturation temperature of CAB, 68 °C, is

DOI: 10.1021/acs.chemmater.6b00193
Chem. Mater. 2016, 28, 2248−2253

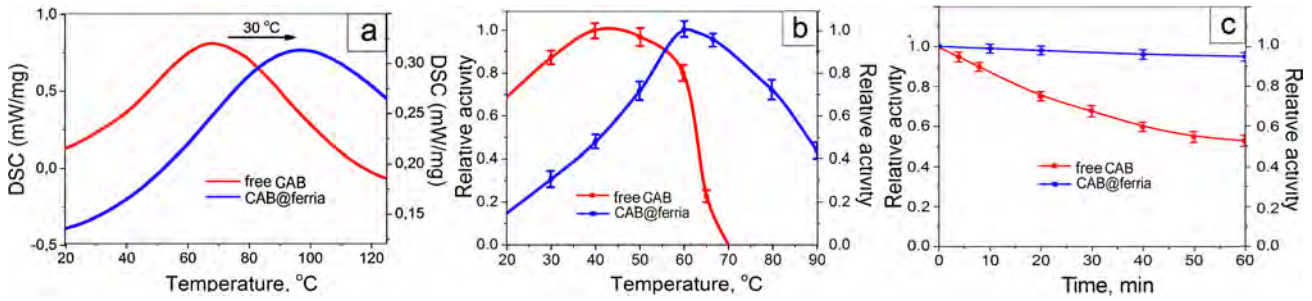

Figure 3. (a) Differential scanning calorimetry (DSC) curves of free CAB and of the CAB@ferria composite. (b) Comparison of the relative enzymatic activities of free CAB and CAB@ferria composite. (c) Comparison of the relative enzymatic activity of free CAB and CAB@ferria composite after exposure to a temperature of 65 °C for 1 h.

pushed up to 98 °C, which is ~30 °C higher! Following this encouraging observation, we performed a comparative study of the relative enzymatic activity of CAB and CAB@ferria at different temperatures. The results are shown in Figure 3b. It can be seen that (i) the relative activity of the free enzyme reaches its maximum at a temperature of 40 °C, which corresponds to absolute activity of 8 μM min^{-1}, and (ii) above 60 °C, there is a rapid loss of activity down to a full stop at 70 °C. This denaturation temperature is in good agreement with the literature.[22] See Figure 4S in the Supporting Information for specific plots of temperature effects on the kinetics on both free and entrapped CAB). CAB@ferria on the other hand shows a distinctly different behavior: The relative activity of the entrapped enzyme grows continuously up to 60 °C, after which the activity gradually decreases, maintained even at 90 °C, namely, very close to the denaturation point (Figure 3a). The exceptional thermal stability of CAB when entrapped in magnetite (CAB@ferria) is further demonstrated in Figure 3c, where the composite was incubated for a period of 60 min at a temperature of 65 °C (close to the maximum for free enzyme, Figure 3a). It can be seen that, while the free enzyme lost 45% of its initial activity, the entrapped enzyme retained 95% of its efficiency, representing a destruction rate of 0.9% of total enzyme molecules/min for the free CAB, compared to 0.08% of total enzyme-molecules/min for CAB@ferria, that is an increase in thermal stability by a full order of magnitude.

The experimental data of Figure 3b allows one to estimate apparent kinetic parameters of the enzymatic reaction, namely, a pseudo-first-order *p*NPA-hydrolysis. A preliminary estimation was first made by taking the experimental rate constants k' and analyzing them using the classical Arrhenius equation,

$$k' = A' \exp\left(- \frac{E_a'}{RT} \right)$$

By doing so, an apparent activation energy (E_a') and an apparent Arrhenius prefactor (A') can be estimated (here, T is the temperature and R is the gas constant). Figures 4a and 4b show this analysis both for the free CAB (Figure 4a) and for the entrapped CAB (Figure 4b). Two different slopes are evident for the free and the entrapped enzyme—up to the temperature where denaturation commences, and beyond it. The right-hand slope relates to the range where temperature is accelerating the reaction (positive activation energy), while the left slope is the higher temperatures range where the enzyme is destroyed, giving rise to negative slopes; we focus only the former.

The apparent activation energy thus calculated for the free enzyme is 14 kJ mol^{-1} with an Arrhenius prefactor of 0.02 s^{-1}. For the entrapped enzyme, the apparent activation energy is

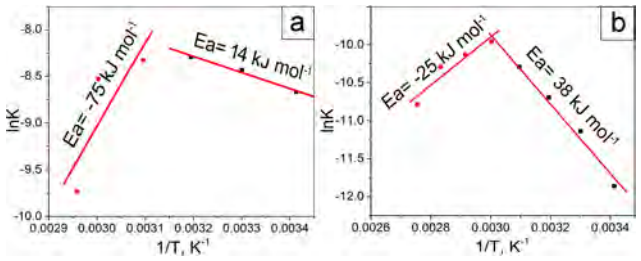

Figure 4. Arrhenius plots of the hydrolysis enzymatic reaction of *p*NPA (a) by free CAB and (b) by CAB@ferria.

higher (38 kJ mol^{-1}), and particularly interesting is the 3 orders of magnitude increase in the prefactor, to 45 s^{-1}. The higher apparent activation energy is a reflection of the well-known diffusional limitations into the pore system of the sol–gel matrix. It is for this reason—and also in order to interpret the increase in the prefactor—that we also took a more advanced model developed for diffusional restricted heterogeneous catalytic process.[29] The general picture remains the same, but with the following corrected values (see the Supporting Information for details): the corrected activation energy is approximately twice the apparent one, namely, 76 kJ mol^{-1}, and the corrected prefactor is smaller, 13 s^{-1}, but still 2.5 orders of magnitude higher, compared to solution. A similar effect of prefactor increase upon entrapment was also reported for the entrapment of CAB in alumina-based composites[14,24] and was interpreted as reflecting the directing effect that pores leading to the enzyme active site have. This phenomenon is possible if the active site of the enzyme is averagely oriented away from the surface and into the pore space. With CAB and ferria, this situation is indeed favorable, because of the following charge considerations. On one hand, at the experimental pH (7.4), the surface of our ferria is positively charged[13] (Figure 7S in the Supporting Information) and therefore repels the neighborhood of the active site of CAB which has large electropositive zones (Figure 6S in the Supporting Information),[30] but attracts the other portions of the protein, which are negatively charged at pH 7.4 (because its isoelectric point of the CAB is 5.9), thus positioning the enzyme in a more favorable orientation towards the incoming substrate molecules.

Generality of the Entrapment and the Stabilization. Following the development of the procedure of entrapment of CAB in magnetite, and the observation of enhanced thermal stability of that entrapped enzyme, we have screened over several other enzymes in order to evaluate the generality of these observations. These proteins are ovalbumin (OVA), horseradish peroxidase (HRP), phosphatase (AcP), xylanase

DOI: 10.1021/acs.chemmater.6b00193
Chem. Mater. 2016, 28, 2248–2253

(XY), and proteinase (PR), all (as mentioned in the Introduction), having specific applications in medicine and in biotechnology. Figure 5 shows that the stabilization effect is

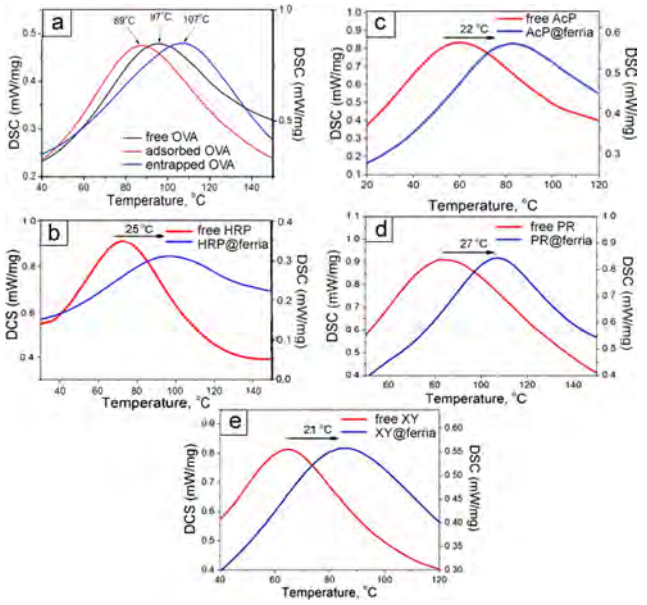

Figure 5. DSC shifts upon thermal denaturation of the free protein, compared to the entrapped protein: (a) ovalbumin (adsorbed OVA is shown as well), (b) horseradish peroxidase, (c) acid phosphatase, (d) proteinase, and (e) xylanase.

general. For OVA@ferria (Figure 5a), the denaturation temperature is higher, compared to the free protein, by 10 °C. Also shown in this figure is the known destabilization of proteins upon adsorption on oxides.[28] The difference in the denaturation temperatures between the destabilized and stabilized enzymes, upon adsorption and entrapment, respectively, is an important manifestation of the inherent differences between these two heterogenization methods. For AcP@ferria, this difference is 22 °C, leading to a 82 °C denaturation temperature of the stabilized enzyme (Figure 5c); for HRP@ferria, the stabilization leads to a temperature that is 25 °C higher (Figure 5b); for PR@ferria, it is elevated by 27 °C (Figure 5d); and for XY@ferria, it is elevated by 21 °C (Figure 5e). Kinetics analyses similarly confirm this generality, and two typical examples are shown in Figure 6, for the two therapeutic enzymes, HRP and AcP. Specifically, for HRP, after 1 h of incubation at 65 °C, the relative activity of the free enzyme dropped to 5% of the initial activity, while the composite material still showed 75% of the enzymatic activity measured prior to heating; and for AcP, after 1 h of heating the

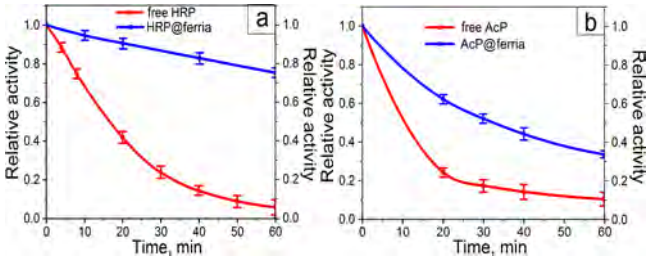

Figure 6. Comparison of the relative of the enzymatic activity of (a) free HRP and HRP@ferria composite; (b) free AcP and AcP@ferria.

activity of free enzyme was 10 times lower (the remaining activity was 10% of the initial one), while the activity of the entrapped enzyme was at 33% of its initial activity.

Magnetic Properties. Obviously, a key property of these entrapped enzymes is that they are magnetically responsive (Figure 7a). Because of the simplicity of the composition and

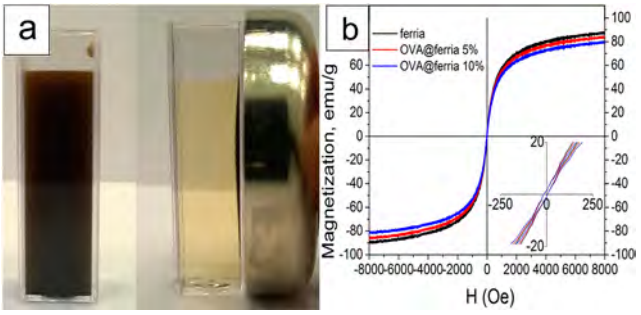

Figure 7. (a) Magnetic manipulation with CAB@ferria. (b) Magnetization curves of OVA@ferria at different protein loadings. The absence of hysteresis loop is showed in the zoomed area.

the absence of coupling agents and stabilizing compounds, the magnetic moments of the obtained materials are very high. As described above, in our case, the average particle size of the magnetite is ∼10 nm (see Figure 2b and Figure 1S in the Supporting Information) and the resulting superparamagnetic behavior is clearly evident (Figure 7b) by the complete absence of hysteresis. The magnetic moment obtained at 6000 Oe amounts to 88 emu/g for the pure magnetite matrix. Entrapment of OVA as a model protein only slightly reduced the magnetic moment to 80 emu/g at 10 wt % loading (Figure 7b).

CONCLUSIONS

In this study, we developed and demonstrated, for the first time, an entrapment methodology of proteins within magnetite sol−gel matrixes. The key has been the use of the newly developed magnetite hydrosol synthesis that does not employ stabilizers and is carried out at a neutral pH. Taking CAB as a model system, we observed enhanced thermal stability of the entrapped protein and a shift of the denaturation temperature to a higher value. This effect was also shown for five additional enzymes of therapeutical and industrial importance. Entrapment of the enzymes not only maintained the biocatalytic activity but allowed one to perform the enzymatic reactions at temperatures higher than the denaturation temperatures of the free enzymes. These findings open up a new methodology for the preparation of magnetic-responsive enzymatic catalysis. Such materials provide new options and possibilities for therapeutic agents or heterogeneous enzymatic reaction catalysts. The capability of moving and positioning the material by imposing a magnetic field also facilitates applications of enzymes in these two fields. From a medical point of view, thermal stability of proteins is of significant importance, and the biocompatibility and injectability make these composites even more interesting. The approach we developed is general: with minimum adaptation, it is possible to create bioactive magnetic composites with almost any enzyme. In summary, we believe that our report provides conclusive evidence that sol−gel-derived ferria is a matrix worth attention as a stabilizing, magnetic, injectable biocarrier of enzymes and other functional proteins.

DOI: 10.1021/acs.chemmater.6b00193
Chem. Mater. 2016, 28, 2248−2253

■ ASSOCIATED CONTENT

Supporting Information

The Supporting Information is available free of charge on the ACS Publications website at DOI: 10.1021/acs.chemmater.6b00193.

HR-SEM images, IR-ATR spectra, surface analysis by N_2sorption, experimental data concerning enzymatic reaction at different temperatures, equations for kinetic parameters calculation and CAB molecule electrostatic potential distribution (PDF)

■ AUTHOR INFORMATION

Corresponding Author

*E-mail: vinogradoffs@mail.ru.

Notes

The authors declare no competing financial interest.

■ ACKNOWLEDGMENTS

This work was supported by the grant of Russian Science Foundation No. 16-13-00041. DSC measurements were supported by the russian president grant MK-9109.2016.3. Electronic microscope measurements were performed in Nanocharacterisation Unit of Hebrew University, Jerusalem.

■ REFERENCES

(1) Avnir, D.; Coradin, T.; Lev, O.; Livage, J. Recent bio-applications of sol−gel materials. *J. Mater. Chem.* **2006**, *16*, 1013−1030.

(2) Mohidem, N. A.; Bin Mat, H. Catalytic activity and stability of laccase entrapped in sol−gel silica with additives. *J. Sol−Gel Sci. Technol.* **2012**, *61*, 96−103.

(3) Frenkel-Mullerad, H.; Ben-Knaz, R.; Avnir, D. Preserving the activity of enzymes under harsh oxidizing conditions: sol−gel entrapped alkaline phosphatase exposed to bromine. *J. Sol−Gel Sci. Technol.* **2014**, *69*, 453−456.

(4) Biró, E.; Budugan, D.; Todea, A.; Péter, F.; Klébert, S.; Feczkó, T. Recyclable solid-phase biocatalyst with improved stability by sol-gel entrapment of β-D-galactosidase. *J. Mol. Catal. B: Enzym.* **2016**, *123*, 81−90.

(5) De Matteis, L.; Germani, R.; Mancini, M. V.; Di Renzo, F.; Spreti, N. Encapsulation of chloroperoxidase in novel hybrid polysaccharide-silica biocomposites: Catalytic efficiency, re-use and thermal stability. *Appl. Catal., A* **2015**, *492*, 23−30.

(6) U.S. Department of Health and Human Services, Food and Drug Administration. *Approved Drug Products with Therapeutic Equivalence Evaluations*, 2014.

(7) Wang, Y. Superparamagnetic iron oxide based MRI contrast agents: Current status of clinical application. *Quant. Imaging Med. Surg.* **2011**, *1*, 35−40.

(8) Lu, M.; Suh, K.; Lee, H.; Cohen, M.; Rieves, D.; Pazdur, R. FDA review of ferumoxytol (feraheme) for the treatment of iron deficiency anemia in adults with chronic kidney disease. *Am. J. Hematol.* **2010**, *85*, 315−319.

(9) Lindblad, E. Aluminium adjuvants—In retrospect and prospect. *Vaccine* **2004**, *22*, 3658−3668.

(10) Singh, D.; Singh, S.; Sahu, J.; Srivastava, S.; Singh, M. Ceramic nanoparticles: Recompense, cellular uptake and toxicity concerns. *Artif. Cells, Nanomed., Biotechnol.* **2014**, *44*, 401−409.

(11) Rutenberg, A.; Vinogradov, V.; Avnir, D. Synthesis and enhanced thermal stability of albumins@alumina: towards injectable sol−gel materials. *Chem. Commun.* **2013**, *49*, 5636−5638.

(12) Vinogradov, A. V.; Vinogradov, V. Low-temperature sol−gel synthesis of crystalline materials. *RSC Adv.* **2014**, *4*, 45903−45919.

(13) Drozdov, A.; Ivanovski, V.; Avnir, D.; Vinogradov, V. V. A universal magnetic ferrofluid: Nanomagnetite stable hydrosol with no added dispersants and at neutral pH. *J. Colloid Interface Sci.* **2016**, *468*, 307−312.

(14) Vinogradov, V.; Avnir, D. Exceptional thermal stability of therapeutical enzymes entrapped in alumina sol−gel matrices. *J. Mater. Chem. B* **2014**, *2*, 2868−2873.

(15) Vinogradov, V.; Avnir, D. Exceptional thermal stability of industrially-important enzymes by entrapment within nano-boehmite derived alumina. *RSC Adv.* **2015**, *5*, 10862−10868.

(16) Volodina, K.; Solov'eva, N.; Vinogradov, V.; Sobolev, V.; Vinogradov, A.; Vinogradov, V. A synergistic biocomposite for wound healing and decreasing scar size based on sol−gel alumina. *RSC Adv.* **2014**, *4*, 60445−60450.

(17) Vinogradov, V.; Vinogradov, A.; Sobolev, V.; Dudanov, I.; Vinogradov, V. Plasminogen activator entrapped within injectable alumina: A novel approach to thrombolysis treatment. *J. Sol-Gel Sci. Technol.* **2015**, *73*, 501−505.

(18) Chapurina, Y.; Vinogradov, V.; Vinogradov, A.; Sobolev, V.; Dudanov, I.; Vinogradov, V. Synthesis of Thrombolytic Sol−Gel Coatings: Toward Drug-Entrapped Vascular Grafts. *J. Med. Chem.* **2015**, *58*, 6313−6317.

(19) Sun, Y.; Duan, L.; Guo, Z.; DuanMu, Y.; Ma, M.; Xu, L.; Zhang, Y.; Gu, N. An improved way to prepare superparamagnetic magnetite-silica core−shell nanoparticles for possible biological application. *J. Magn. Magn. Mater.* **2005**, *285*, 65−70.

(20) Xu, J.; Ao, Y.; Fu, D.; Yuan, C. Low-temperature preparation of anatase titania-coated magnetite. *J. Phys. Chem. Solids* **2008**, *69*, 1980−1984.

(21) Pogorilyi, R.; Melnyk, I.; Zub, Y.; Seisenbaeva, G.; Kessler, V.; Shcherbatyik, M.; Kosak, A.; Lobnik, A. Urease adsorption and activity on magnetite nanoparticles functionalized with monofunctional and bifunctional surface layers. *J. Sol−Gel Sci. Technol.* **2013**, *68*, 447−454.

(22) Lindskog, S. Structure and mechanism of carbonic anhydrase. *Pharmacol. Ther.* **1997**, *74*, 1−20.

(23) Sun, M.; Alkon, D. Carbonic anhydrase gating of attention: memory therapy and enhancement. *Trends Pharmacol. Sci.* **2002**, *23*, 83−89.

(24) Vinogradov, V.; Avnir, D. Enzyme renaturation to higher activity driven by the sol−gel transition: Carbonic anhydrase. *Sci. Rep.* **2015**, *5*, 14411.

(25) Al Taira, M.; Merrick, G.; Wallner, K.; Dattoli, M. Reviving the acid phosphatase test for prostate cancer. *Oncology* **2007**, *21*, 1003−1010.

(26) Choct, M. Enzymes for the feed industry: past, present and future. *World's Poult. Sci. J.* **2006**, *62*, 5−16.

(27) Kirk, O.; Borchert, T. V.; Fuglsang, C. C. Industrial enzyme applications. *Curr. Opin. Biotechnol.* **2002**, *13*, 345−351.

(28) Nakanishi, K.; Sakiyama, T.; Imamura, K. On the adsorption of proteins on solid surfaces, a common but very complicated phenomenon. *J. Biosci. Bioeng.* **2001**, *91*, 233−244.

(29) Fogler, H. S. *Elements of Chemical Reaction Engineering*, 4th Edition: Prentice Hall: Englewood Cliffs, NJ, 2015; pp 845−846.

(30) Saito, R.; Sato, T.; Ikai, A.; Tanaka, N. Structure of bovine carbonic anhydrase II at 1.95 Å resolution. *Acta Crystallogr., Sect. D: Biol. Crystallogr.* **2004**, *60*, 792−795.

DOI: 10.1021/acs.chemmater.6b00193
Chem. Mater. 2016, 28, 2248−2253